ISSN 0965-5425, Computational Mathematics and Mathematical Physics, 2015, Vol. 55, No. 8, pp. 1370–1380. © Pleiades Publishing, Ltd., 2015.
Original Russian Text © K.V. Brushlinskii, A.N. Kozlov, V.S. Konovalov, 2015, published in Zhurnal Vychislitel'noi Matematiki i Matematicheskoi Fiziki, 2015, Vol. 55, No. 8, pp. 1405–1416.

In blessed memory of Professor A.P. Favorskii

Numerical Models of Steady-State and Pulsating Flows of Self-Ionizing Gas in Plasma Accelerator Channels

K. V. Brushlinskii, A. N. Kozlov, and V. S. Konovalov

Keldysh Institute of Applied Mathematics, Russian Academy of Sciences, Miusskaya pl. 4, Moscow, 125047 Russia
e-mail: andrey-n-kozlov@mail.ru

Received February 9, 2015

Abstract—This paper continues the series of numerical investigations of self-ionizing gas flows in plasma accelerator channels with an azimuthal magnetic field. The mathematical model is based on the equations of dynamics of a three-component continuous medium consisting of atoms, ions, and electrons; the model is supplemented with the equation of ionization and recombination kinetics within the diffusion approximation with account for photoionization and photorecombination. It also takes into account heat exchange, which in this case is caused by radiative heat conductance. Upon a short history of the issue, the proposed model, numerical methods, and results for steady-state and pulsating flows are described.

DOI: 10.1134/S0965542515080059

Keywords: plasma accelerator, plasma and gas flows, ionization process, mathematical models, steady-state and pulsating flows.

INTRODUCTION

The present paper is a part of a large series of studies on mathematical modeling of complex physical processes related to plasma technology and constant interest in astrophysics. While studying these phenomena during many years, the authors maintained fruitful contacts with Favorskii and his teachers Tikhonov, Samarskii, Kurdyumov, and his coauthor Degtyarev and associates Tishkin, Shashkov, and others. Below, we briefly mention related issues in our studies and uses of numerical methods proposed by those researchers.

This paper is devoted to numerical models and computation of the gas ionization process and plasma acceleration in the electromagnetic field formed in coaxial channels of plasma accelerators. The development of such accelerators had been conducted for many years at the initiative and under the guidance of Morozov. The record parameters of acceleration and generation of high-energy plasma flows were achieved in the cooperation of several research institutions of Moscow, St. Petersburg, Troitsk, Kharkov, and Minsk within the development of the quasi-steady high-current plasma accelerator (QHPA) [1–3]. An acceleration of ~400 km/s occurs in the main nozzle channel with a diameter of 50 cm formed by two coaxial electrodes. The plasma is injected into this channel from several small accelerators (input ionization cameras) arranged around it, where the gas is ionized. The ionization process is complex and poorly understood. In contrast to the flow of completely ionized plasma in a channel, which practically occurs in a quasi-stationary mode or, under some idealization, also in the stationary mode, both steady-state and nonstationary pulsating modes are observed in the flows of self-ionizing gas. Although the analysis of physical conditions under which one or the other mode occurs yielded some preliminary result, this problem remains unsolved. In addition to theoretical and experimental works, it is studied by numerical simulation; the present paper uses numerical simulation.

In earlier studies, some mathematical models of the ionization processes were proposed in terms of mechanics of continua, i.e. in terms of magnetic hydrodynamics (MHD) and its generalizations in the quasi-one-dimensional (hydraulic) approximation, which consider flows in narrow nozzle channels. For simplicity and uniformity, these approximations assume that the gas entering the channel is weakly ionized, i.e., it has a small but nonzero electrical conductivity. A simple MHD model assumes a jump-like dependence of the conductivity σ on the temperature T: for $T < T^*$, where T^* is a given value assigned to ionization, the conductivity $\sigma = \sigma_1$ is small (which corresponds to gas), and for $T < T^*$ $\sigma = \sigma_2 \gg \sigma_1$, and

the medium must be considered as plasma in this case (see [4, 5]). In computations of nonstationary MHD flows, steady-state modes are observed if the jump $\sigma_2 - \sigma_1$ is bounded above, while pulsating modes are observed when this condition is violated. Another model deals with three-component continuous medium consisting of neutral atoms, ions, and electrons whose ratio (i.e., ionization level) obeys the laws of local thermodynamic equilibrium described by the Saha equation. In the computations performed in the quasi-one-dimensional case, either steady-state or pulsating flows are also observed, which differ from each other in the ratio $J_p^2/\dot{m}$ of the total current squared to the mass flow in the channel—in steady-state modes this ratio exceeds a certain fixed value determined by computations (see [6–8]). Computations of two-dimensional flows with a nontrivial dependence on the transverse coordinate are described in [9], where the abovementioned pattern is also observed.

In the two models mentioned above, the ionization front turned out to be too diffuse. A narrow front, which better agrees with experimental data, was obtained in the numerical model described in [10] in which the equations of dynamics of the three-component continuous medium are supplemented with the kinetic equation of ionization and recombination within a modified diffusion approximation (see [11]). In this model, the structure of atomic energy levels is taken into account and the nonequilibrium nature of processes is revealed. A well-defined deviation from ionization-recombination equilibrium on the ionization front was observed in the computations, which significantly changed our understanding of the process under study. For steady-state flows, the basics of the theory of processes on the ionization front were developed (see [12]).

Both in experimental and numerical studies, one can notice pulsating flow modes characterized by large temperature variations. Heated conductive plasma layers periodically appear on the ionization front and move along the channel while cooling down and spreading. These flow modes seem to have the same mathematical (in terms of the models under consideration) and physical nature as the high-temperature layers that periodically occur in plasma cylinder expansion models (see [13]) and in models of plasma acceleration in a pulsed railgun accelerator (see [14]). They were discovered in numerical experiments by a group of researchers that included Favorskii under the guidance of Tikhonov and Samarskii and referred to as *T-layers*. In the opinion of these authors, a significant role in the model of these phenomena is played by the nonlinear dependence of plasma conductivity on its temperature.

The further investigation of the ionization process requires the radiative heat exchange to be taken into account (e.g., see [15, 16]). Its influence on the flows was studied using models of different level of complexity in [17], including the mechanism of spectrum line broadening (see [18]). In simple cases, it suffices to use the radiative heat conductance approximation, which is justified by the fact that the medium is optically nontransparent for the radiation in the lines that make the major contribution to the total radiation field. The total heat flux is also due to the electron and atomic heat conductance.

In this paper, we describe numerical investigations of the nonstationary nonequilibrium ionization process in the quasi-one-dimensional flow model with account for the radiative heat conductance and ionization and recombination kinetics.

1. STATEMENT OF THE PROBLEM ON SELF-IONIZING GAS FLOW

Schematically, the plasma accelerator channel consists of two coaxial electrodes connected to an electric circuit. Neutral gas is injected between the electrodes (Fig. 1). If there is voltage between the electrodes, gas breakdown occurs and an ionization front is formed.

The MHD model of the flow of self-ionizing gas is based on the equation of transfer for the three-component medium (see [19]) consisting of atoms, ions, and electrons and on the magnetic field diffusion equation, which is a consequence of Maxwell's equations and Ohm's law if the inertia of electrons and the displacement current are neglected.

The ionization process is studied for hydrogen, which is often used in experiments. The masses of atoms and ions are identical: $m_a = m_i = m$. It is known from experimental data that the temperature at the ionization front increases up to 1–3 eV. The concentration of the gas entering the channel is supposed to be sufficiently high—$n = 10^{16} - 10^{18}$ cm^{-3}. Such a medium is quasi-neutral, i.e., $n_i = n_e$. The velocities of the medium components can be assumed to be identical: $\mathbf{V}_i = \mathbf{V}_e = \mathbf{V}_a = \mathbf{V}$. In addition, the experimental data and estimates suggest that we may consider the case of single-temperature mixture: $T_a = T_i = T_e = T$.

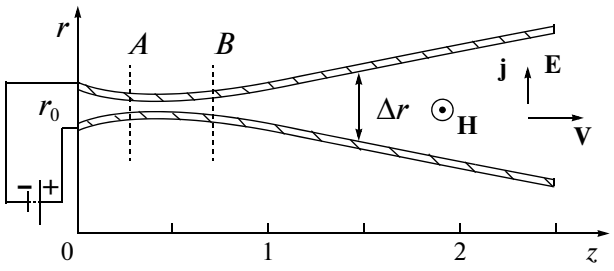

Fig. 1. Schematic of the plasma accelerator channel.

Simple transformations of the initial transfer equations for the three-component medium and the equation of the magnetic field diffusion with regard to the above assumptions yield the following modified system of MHD equations supplemented with the equation of ionization and recombination kinetics:

$$\frac{\partial n_e}{\partial t} + \operatorname{div}(n_e\mathbf{V}) = n_a n_e \beta_{\text{ion}} - n_e^2 n_i \alpha_{\text{rec}} + n_a \beta_\omega - n_e n_i a_\omega, \tag{1.1}$$

$$\frac{\partial \rho}{\partial t} + \operatorname{div}(\rho\mathbf{V}) = 0, \quad \rho\frac{d\mathbf{V}}{dt} + \nabla P = \frac{1}{c}\mathbf{j}\times\mathbf{H}, \tag{1.2}$$

$$\rho\frac{d\varepsilon}{dt} + P\operatorname{div}\mathbf{V} = \frac{\mathbf{j}^2}{\sigma} - \operatorname{div}\mathbf{q} - \operatorname{div}\mathbf{W}, \tag{1.3}$$

$$\frac{\partial \mathbf{H}}{\partial t} = \operatorname{curl}(\mathbf{V}\times\mathbf{H}) - c\operatorname{curl}\frac{\mathbf{j}}{\sigma}, \tag{1.4}$$

$$\mathbf{q} = -\kappa_{e\to a}\nabla T, \quad \mathbf{W} = -\kappa_{\text{rad}}\nabla T, \quad P = P_a + P_i + P_e = (1+\alpha)(c_P - c_V)\rho T, \quad \varepsilon = (1+\alpha)c_V T + \varepsilon_I,$$

$$\alpha = \frac{n_e}{n_a + n_i}, \quad \mathbf{j} = \frac{c}{4\pi}\operatorname{curl}\mathbf{H}, \quad \frac{d}{dt} = \frac{\partial}{\partial t} + (\mathbf{V},\nabla).$$

Here, $\rho = mn_{\text{tot}}$ is the density of heavy particles, $n_{\text{tot}} = n_a + n_i$ is the total concentration of heavy particles, α is the degree of ionization, $\mathbf{q}$ is the heat flux, $\kappa_{e\to a}$ is the electron-atomic heat conductiance, $\mathbf{W}$ is the radiation energy flux, κ_{rad} is the radiation heat conductance, and P is the total pressure. The Joule heating $Q_{ei} = \mathbf{j}^2/\sigma$ in Eq. (1.3) for the internal energy considerably exceeds the heat generated due to friction with other components. The internal energy per unit of mass ε includes the additional term $\varepsilon_I = \varsigma\alpha I/m_i$, which is responsible for the loss of energy for ionization, where I is the atom ionization energy. The recombination α_{rec} and ionization β_{ion} coefficients in Eq. (1.1) and the process related to photoionization and photorecombination are responsible for the generation and loss of free electrons. The medium electrical conductivity in Eqs. (1.3) and (1.4) is $\sigma = e^2 n_e/m_e\nu_e$, where the average frequency of collisions of an electron with other particles ν_e is composed of the frequencies of collisions with atoms and ions:

$$\nu_e = \nu_{ea} + \nu_{ei}, \quad \nu_{ea} = n_a\langle V_e\rangle S_{ea}, \quad \nu_{ei} = n_i\langle V_e\rangle S_{ei}; \tag{1.5}$$

here, S_{ea} and S_{ei} are the effective collision sections (see [20]).

The main heat transfer mechanisms depend on the medium state. In the case of large degrees of ionization, a significant role in the total heat transfer is played by the classical electron heat conductance across the magnetic field. At low degrees of ionization, atomic heat conductance makes a noticeable contribution. The total thermal conductivity coefficient is determined by a unified formula (see [20]) that describes the transition from the weakly ionized state to greater degrees of ionization.

The radiative heat conductance (see [15]) is $\kappa_{\text{rad}} = \frac{16}{3} C_{\text{sb}} L_{\text{cp}} T^3$, where C_{sb} is the Stefan–Boltzmann constant. The mean path of photons

$$L_{\text{cp}} \approx \frac{m_e c}{\pi e^2} \frac{\Delta\omega}{n_k f_{kl}}, \quad n_k = n_1 \approx n_a$$

is determined based on the Doppler broadening of spectrum lines $\Delta\omega = \omega_{kl} V/c$, where $\omega_{kl} = 2\pi c/\lambda_{kl}$ and f_{kl} are the spectral frequency and the oscillator strength, for example, for the Lyman α-line of hydrogen plasma. Estimations and computations show that the role of heat conductance is by and large insignificant. The statement of the problem includes boundary conditions on the electrodes, entry, and exit of the accelerator channel.

2. KINETICS OF EXCITED STATE POPULATION

Plasma is a multicomponent medium. By interacting between themselves, with the plasma radiation and fields, the components can change their energy state thus affecting the energy balance of the medium and participate in the formation of other components through the processes of ionization and recombination. Therefore, in the description of plasma dynamics, we face the problem of determining the medium composition.

In the state of thermodynamic equilibrium, the plasma composition is determined by the value of thermodynamic parameters. The low-temperature plasma is described by Boltzmann's statistics. Atoms and ions can be in the ground or excited states in which the concentrations of particles are related by Boltzmann's equation. In the local thermodynamic equilibrium approximation, the concentrations of plasma components (electrons, ions, and atoms) are determined by the Saha equation

$$\frac{n_e n_i}{n_a} = K_1 = 2\frac{\Sigma_i}{\Sigma_a}\left(\frac{2\pi m_e k_b T}{h^2}\right)^{3/2} \exp\left(-\frac{E_1}{k_b T}\right), \tag{2.1}$$

where E_1 is the ground state binding energy, which is equal to the ionization energy; Σ_i and Σ_a are the statistical sums; and K_1 is the ionization equilibrium constant. Under the quasi-neutrality condition $n_i = n_e$, Eq. (2.1) can be used to find the degree of ionization. In this case, the local thermodynamic equilibrium approximation assumes the direct ionization from the ground state and the inverse recombination process.

As a matter of fact, a bound electron in an atom can transit from level to level on a complex path before it reaches the continuum or conversely the ground state. In the general case, the system of equations of level-by-level kinetics must be solved that determine the concentration of excited particles in the kth state. The solution of this system is a nontrivial task. For this reason, the quasi-stationary approximation is sometimes used, under which the population of the kth atom state has time to adjust to such relatively slowly varying plasma parameters as temperature and concentration.

There are several approaches to the approximate analytical calculation of level population. One such approach uses the smearing of the discrete energy spectrum. In the corresponding diffusion approximation, the balance system of equations is reduced to an equation for populations $n(E)$ considered as a continuous function of time. This approach is valid for highly excited states separated by small energy intervals. The quasi-continuous transport in the energy space is characterized by the flux $j(E)$, which depends on the density of particles, gradient, and the corresponding coefficients in the flux representation by a series. Based on the transport continuity, the divergence of this flux is equal to the change in the concentration of particles with the energy E according to the Fokker–Planck equation, which is used for finding the recombination coefficient and determining the nonequilibrium distribution of populations.

In the single-quantum approximation, the electron motion is considered in the atom energy space assuming that the energy levels are discrete. The probability of collisional transitions depends on the energy level difference as $W_{km} \sim (E_k - E_m)^{-4}$. For this reason, transitions between adjacent levels are most probable. In the single-quantum approximation, we have for the electron flux in the energy space between the levels k and $k-1$ as a result of collision processes

$$j = n_k W_{k,k+1} - n_{k+1} W_{k+1,k}. \tag{2.2}$$

A drawback of the single-quantum approximation is that only transitions between the adjacent levels are taken into account. This drawback is overcome in the modified diffusion approximation. This approximation also takes into account the discreteness of the atom energy levels, and the transport of a bound electron caused by collision processes is considered as diffusion in the discrete space. The difference Fokker–Planck equation is derived (see [11]), which, in the limit case of merging levels, turns into the differential equation. The difference Fokker–Planck equation corresponds to the collision flux, the form of which coincides with expression (2.2) for the flux in the single-quantum approximation. In the modified diffusion approximation, the probabilities $W_{k,k+1}$ should be replaced with the effective probabilities of single-quantum transitions $Z_{k,k+1}$ in which the contributions of different collisional transitions are summarized.

Using the quantum-mechanical rule for summing transition probabilities, we can calculate the effective transition probabilities and average them over the Maxwell distribution of free electrons. As a result, we obtain the following relation for $k > 1$:

$$Z_{k,k+1} = \frac{4\sqrt{2\pi}\Lambda_k e^4 n_e E_{k-1}}{\sqrt{m_e k_b T_e}\,(E_{k-1} - E_{k+1})(E_k - E_{k+1})} \exp\left(-\frac{E_k - E_{k+1}}{k_b T_e}\right); \tag{2.3}$$

here, Λ_k is the Coulomb logarithm of the bound electron. For the effective probabilities, the principle of detailed balance $n_k^0 Z_{k,k+1} = n_{k+1}^0 Z_{k+1,k}$ holds. Following [11], we can finally obtain the stepwise recombination coefficient

$$\alpha_{\text{cm}}^{-1} = 2\Sigma_i n_e \frac{(2\pi m_e k_b T_e)^{3/2}}{h^3} \sum_{k\geq 1} \frac{\exp(-E_k/k_b T_e)}{g_k Z_{k,k+1}}, \tag{2.4}$$

where g_k is the statistical weight. The stepwise ionization coefficient β_{cm} is related to α_{cm} as

$$\beta_{\text{cm}} = K_1 \alpha_{\text{cm}}, \tag{2.5}$$

where the ionization equilibrium constant K_1 is calculated using (2.1).

The quantities β_{cm} and α_{cm} determined by formulas (2.3)–(2.5) make it possible to find the rates of stepwise ionization and recombination processes. In distinction from the diffusion approximation and a number of interpolation formulas in [11], the relations discussed above, in which the contributions of different levels within the ionization and recombination kinetics are summarized, were successfully used to calculate the flow with the formation of a narrow ionization front corresponding to experimental data.

3. QUASI-ONE-DIMENSIONAL FLOW MODEL

In self-ionizing gas flows, of major interest is the dependence of flow parameters on the longitudinal coordinate of the accelerator channel. The variation of variables in the transverse or radial direction is insignificant and can be neglected. Therefore, we may restrict ourselves to the quasi-one-dimensional approximation (e.g., see [21, 4, 5]) and consider the flow in a narrow cylindrical tube of the channel of given section. In this case, the functions to be found are averaged over the transverse section of the channel and satisfy equations that include two independent variables—the time t and the spatial coordinate z along the channel. We assume that the average characteristic channel radius $r = r_0$ is constant. The equations include the area of the channel transverse section $f(z) = 2\pi r_0 \Delta r(z)$, where $\Delta r(z)$ is the gap between the electrodes.

Figure 1 shows the projection of the coaxial electrodes on the plane (r, z). Let the external electrode be the cathode, and the internal one be the anode. The corresponding directions of the current, electric field, and azimuthal magnetic field are shown in this figure. The magnetic field is perpendicular to the direction of the electric current and the plane of Fig. 1. In the narrowest part of the channel (the interval AB in Fig. 1), the gas is ionized and forms a narrow front. Behind the front, the plasma accelerates due to the Ampère force.

In the quasi-one-dimensional approximation, the ionization process is described by the extended system of MHD equations (see [10, 12]), which can be represented in dimensionless form. Introduce the

notation $V = V_z$ and $H = H_\varphi$. Taking into account the equation of ionization and recombination kinetics, we have

$$\frac{\partial n_e f}{\partial t} + \frac{\partial n_e V f}{\partial z} = f\tilde{\Gamma}_e, \quad \tilde{\Gamma}_e = n_a n_e \tilde{\beta}_{\text{ion}} - n_e^2 n_i \tilde{\alpha}_{\text{rec}} + \tilde{\beta}_\omega n_a - n_e n_i \tilde{\alpha}_\omega,$$
$$\frac{\partial \rho f}{\partial t} + \frac{\partial \rho V f}{\partial z} = 0, \quad \rho = n_a + n_i,$$
$$\frac{\partial \rho V f}{\partial t} + \frac{\partial (\rho V f) V}{\partial z} = -f\frac{\partial}{\partial z}\left(P + \frac{H^2}{2}\right), \quad P = \frac{\beta}{2}(1+\alpha)\rho T,$$
$$\frac{\partial \rho \varepsilon f}{\partial t} + \frac{\partial (\rho \varepsilon f) V}{\partial z} = -P\frac{\partial V f}{\partial z} + f\nu\left(\frac{\partial H}{\partial z}\right)^2 - \frac{\partial f q}{\partial z}, \tag{3.1}$$
$$\frac{\partial H f}{\partial t} + \frac{\partial H V f}{\partial z} = \frac{\partial}{\partial z}\left(\nu f \frac{\partial H}{\partial z}\right),$$
$$\varepsilon = \frac{\beta(1+\alpha)T}{2(\gamma-1)} + \frac{\beta}{2}\varsigma\alpha T^*, \quad n_e = n_i, \quad \alpha = \frac{n_e}{\rho}, \quad n_a = (1-\alpha)\rho, \quad q = -\tilde{\kappa}\frac{\partial T}{\partial z},$$
$$\nu = 1/\sigma_0 = 1/\sigma_1 + 1/\sigma_2, \quad \sigma_1 = \alpha\sigma_{10}/(1-\alpha)\sqrt{T}, \quad \sigma_2 = \sigma_{20}T^{3/2}.$$

At the entry $z = 0$, $\rho = 1$, $T = 1$, $H = 1$, and $\alpha = \alpha_{\text{in}}$ are given. At the exit of the accelerator $z = z_{\text{out}}$, the boundary conditions correspond to free outflow. As the measurement units, we use the dimensional parameters at the entry n_0 ($\rho_0 = mn_0$), T_0, H_0, and the length of the channel or its part L. The characteristic magnetic field $H_0 = 2J_p/cr_0$ is determined by the discharge current in the system J_p. Using these quantities, the units of pressure $H_0^2/4\pi$, velocity $V_0 = H_0/\sqrt{4\pi\rho_0}$, time L/V_0, and electric field $E_0 = H_0V_0/c$ are formed. The dimensionless parameters in (3.1) are

$$\beta = 8\pi P_0/H_0^2, \quad (P_0 = k_b n_0 T_0), \quad \nu = c^2/4\pi L V_0 \sigma, \quad T^* = I/k_b T. \tag{3.2}$$

The dimensionless conductivity or the magnetic Reynolds number $\sigma_0 = \text{Re}_m = 1/\nu$ include the quantities σ_{10} and σ_{20}, which are represented in terms of the initial dimensional parameters and physical constants using (1.5). The dimensionless values of the heat conductivity $\tilde{\kappa}$, ionization and recombination coefficients $\tilde{\beta}_{\text{ion}}$, $\tilde{\alpha}_{\text{rec}}$, $\tilde{\beta}_\omega$, and $\tilde{\alpha}_\omega$ in (3.1) are determined in terms of the dimensional constants. The internal energy equation is replaced with the equation for entropy.

The first equation in (3.1) describes the rate of electron production with regard to various processes described by the right-hand side. Estimates of probabilities of different processes show that the major factor causing ionization and recombination in the case of sufficiently dense low-temperature plasma is the interaction of electrons with atoms and ions corresponding to the following elementary direct and inverse processes: $A_k + e \leftrightarrow A_m + e$ (excitation and deexcitation and $A_k + e \leftrightarrow A^+ + e + e$ (electron collisonal ionization and triple recombination). In addition, there is photoionization and photorecombination $A_k + \hbar\omega \leftrightarrow A^+ + e$.

For hydrogen atoms within the modified diffusion approximation (see [11]), in which the diffusion of the bound electron is considered in the atom's energy space with regard to the fact that its energy levels are discrete, the stepwise recombination coefficient α_{cm} is determined, in accordance to (2.3) and (2.4), by

$$\alpha_{\text{cm}} = \frac{h^3 e^4}{2\pi(m_e k_b T_e)^2 \Sigma_i E_1}\left[\sum_{k\geq l}\frac{(2k+1)}{k^3(k+1)^4}\frac{\exp(-E_{k+1}/k_b T_e)}{\Lambda_k}\right]^{-1}, \tag{3.3}$$

where $E_k = E_1/k^2$ and $E_1 = I = 13.6$ eV $= 2.16\times10^{-11}$ erg for hydrogen atoms.

The total ionization and recombination coefficients include the direct ionization process from the ground state and the inverse recombination process:

$$\beta_{\text{ion}} = \beta_{\text{cm}} + \beta_{\text{st}}, \quad \alpha_{\text{rec}} = \alpha_{\text{cm}} + \alpha_{\text{st}}, \quad \text{where } \beta_{\text{st}} = W_{l,e}/n_e, \quad \alpha_{\text{st}} = (W_{e,l} + A_{el})/n_e.$$

Here, the Einstein coefficient A_{el} determines the probability of spontaneous radiation. The major contribution is made by the stepwise processes in accordance with (3.3) and (2.5).

In addition, we take into account the processes related to photoionization and photorecombination (e.g., see [15]). When the spectral density of the equilibrium radiation or Planck's function are used, the corresponding coefficients in (1.1) and (3.1) are calculated by

$$\beta_\omega = \frac{8\pi I^2 k_b T}{c^2 h^3}\sigma_\omega^0 \exp\left(-\frac{I}{k_B T}\right), \quad \alpha_\omega = \frac{\beta_\omega n_a}{n_e n_i},$$

where $\sigma_\omega^0 = 7.9\times 10^{-18}$ cm^2 is the hydrogen effective photoionization section.

The area of the channel cross-section is specified as $f(z) = 0.3 - 0.8z(1-z)$ for $z \le 1$ and $f(z) = 0.8z - 0.5$ for $1 \le z \le z_{\text{out}} = 3$. The channel is a nozzle of unit length with a linearly expanding socket added on the right (Fig. 1).

4. COMPUTATION TECHNIQUES

The numerical simulation of MHD problems, along with common features characteristic of conventional fluid dynamics, has some specific features discussed, e.g., in [22]. In the numerical model presented in this paper, the hyperbolic part of the MHD equations (e.g., see [23]) is solved using the flux-corrected scheme (see [24]).

The parabolic part of the MHD equations includes the electrical and heat conductivity coefficients, which are highly variable at the ionization front along with the thermodynamic parameters of the medium for the self-ionizing gas flows considered in this paper; the thermodynamic parameters are determined by the magnetic fluid dynamics of the medium. For example, the account for electrical conduction in the equation of magnetic field diffusion for the azimuthal component of the magnetic field $H = H_\varphi$ requires, according to (3.1), a boundary value problem for the equation

$$\frac{\partial Hf}{\partial t} = \frac{\partial}{\partial z}\left(\nu f \frac{\partial H}{\partial z}\right)$$

to be solved. A reliable method for solving problems with strongly varying coefficients is based on the use of the flow variant of the sweep method (see [25]). It was shown in that paper that, in problems with strongly varying coefficients when the conventional sweep method results in the complete loss of accuracy, the flow variant yields high quality and reliable results.

5. NUMERICAL RESULTS FOR SELF-ORGANIZING GAS FLOWS

In experiments on plasma accelerators and in simple ionization models (see [4, 5, 9]), steady-state and pulsating modes were observed, depending on the values of the discharge current and mass flux. Periodic flow modes were also observed in MHD flows with switching off of the electrical conductivity switched off (see [26]).

In the proposed model, two flow modes are also realized. In particular, as the discharge current is decreased, pulsating flows are observed instead of the steady-state ionization process. Figure 2 shows the characteristic distributions of the MHD variables in the pulsating flow at different times $t_1 = 8.8$ (solid lines) and $t_2 = 8.85$ (dashed lines) corresponding to $n_0 = 2.5\times 10^{17}$ cm^{-3}, $T_0 = 500$°K, $J_p = 55kA$, $\alpha_{\text{in}} = 10^{-10}$, $\beta = 0.16$, $T^* = 313$, and $V_0 = 0.7\times 10^6$ cm/s. These values of concentration and temperature at the entry correspond to the range of parameters used in plasma accelerators. We assume that equilibrium weakly ionized gas is fed at the entry of the channel; the degree of ionization α_{in} of this gas is determined by the Saha equation (2.1).

The flow of the self-organizing gas is characterized, on the one hand, by sharp increase in temperature, velocity, and degree of ionization and, on the other hand, by sharp decrease in the density and magnetic field at the ionization front located in the narrowest part of the channel. In distinction from the earlier models, we have much sharper dependences of all the variables at the front within the kinetics and recombination model. This indicates that the description of the ionization process agrees with experiments (e.g., see [27–30]), in which a narrow ionization front is observed. In addition, it is clearly seen in Fig. 2f that the ionization process is nonequilibrium in the neighborhood of the front, which is indicated by a peak of the function $\Gamma = \tilde{\Gamma}_e(z)$ on the right-hand side of the first equation in (3.1).

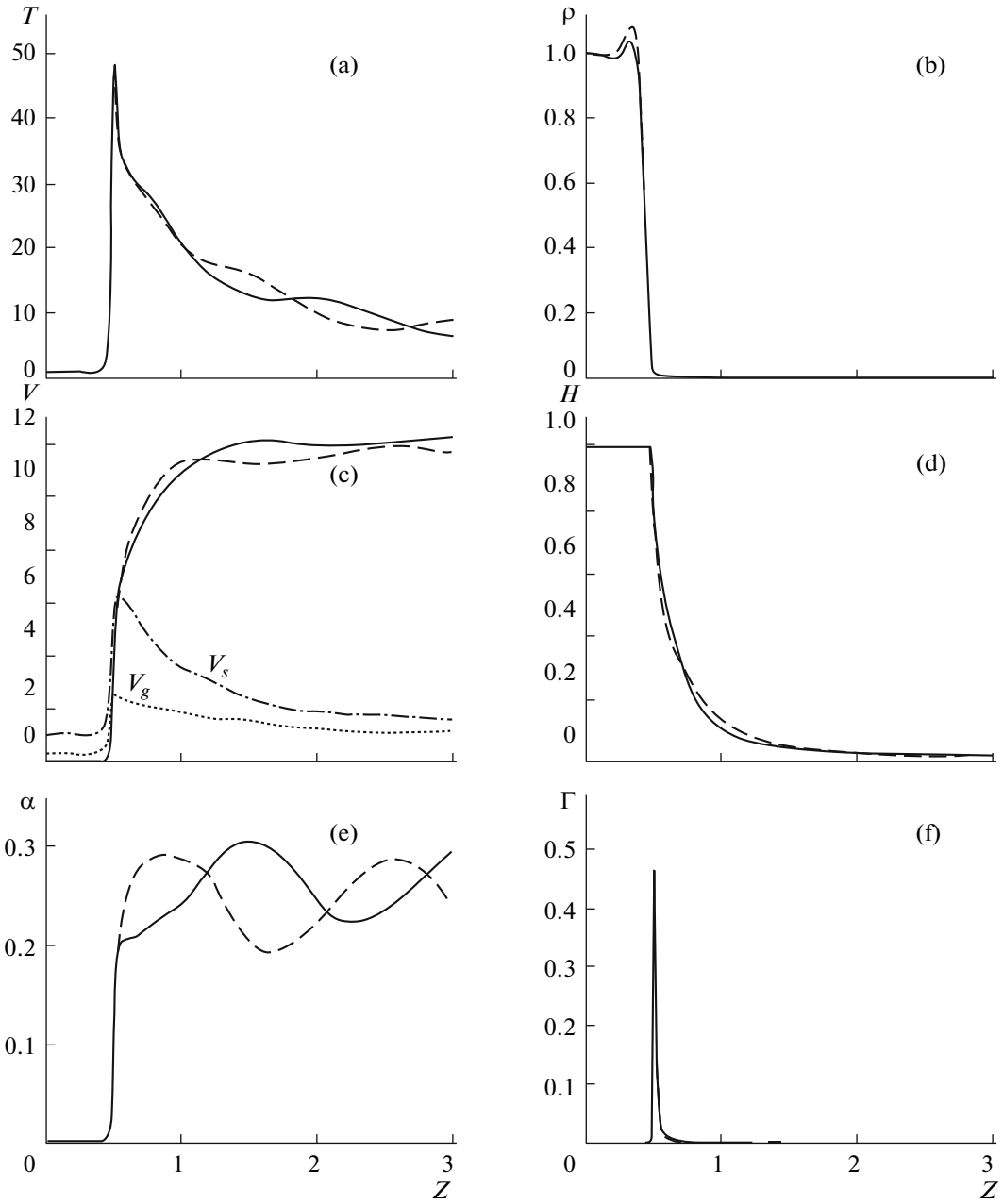

Fig. 2. Distribution of the MHD parameters along the channel in the pulsating flow of the ionizing gas at different times: (a) temperature, (b) density, (c) velocity of the medium, (d) magnetic field, (e) degree of ionization, and (f) deviation from equilibrium.

Pulsating flows of the self-ionizing gas are accompanied by oscillations of all the variables. Figure 3 shows the plots of the temperature and degree of ionization as functions of time for the flow pattern shown in Fig. 2. The values of the quantities are given at the channel exit.

In the process of ionization, the flow velocity in the neighborhood of the front first overcomes the gas dynamic speed of sound $V_g = \sqrt{\gamma P/\rho}$ (the dotted line in Fig. 2c) and then the magneto-gas dynamic speed of sound $V_s = \sqrt{V_g^2 + H^2/\rho}$ (the dot-and-dash line in Fig. 2c). In steady-state flows of the self-ionizing gas, the transonic transition for V_g occurs in the narrowing part of the channel ($z < 0.5$), while the transition through V_s occurs in the most narrow part of the channel $z = 0.5$. In nonstationary flows, the transition through V_g and V_s occurs in the divergent part of the channel at $z \geq 0.5$. This, in particular, explains the

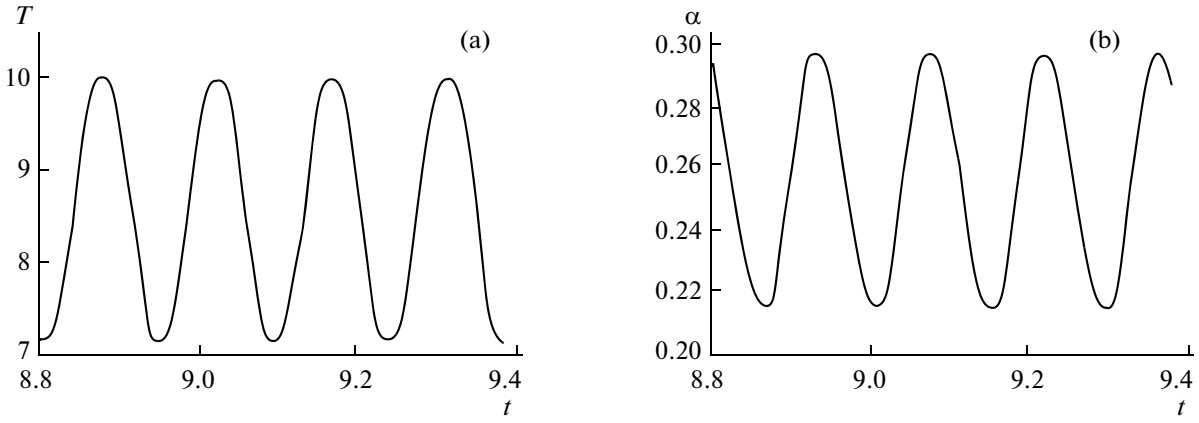

Fig. 3. Time dependences of the parameters in the pulsating flow of ionizing gas: (a) temperature and (b) the degree of ionization.

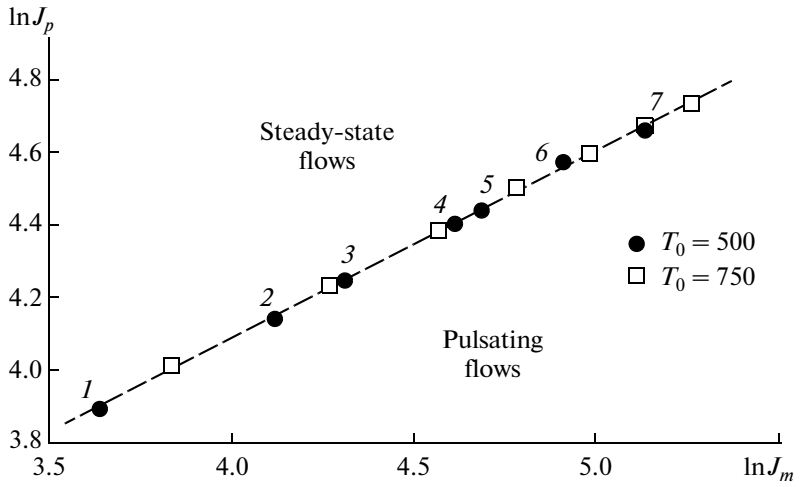

Fig. 4. Boundary between the steady-state and pulsating flows of the ionizing gas.

occurrence of pulsating modes but does not completely explain nonstationary flows, which can also occur due to processes in electric circuits and other factors.

From numerical results, we determined the boundary of transition from pulsating modes to steady-state flows of the self-ionizing gas. This boundary is shown by a dashed line in Fig. 4 in the plane of variables $(\ln J_{\dot m}, \ln J_p)$, where $J_{\dot m} = e\dot m/m_i$ (kA) is the mass flux expressed in the units of current. Above the dashed line, at large values of the discharge current, we have steady-state flows. Below this line, at lower values of the discharge current, nonstationary pulsating modes are observed. Different markers at the boundary correspond to quasi-stationary flows calculated for two values of the temperature $T_0 = 500$°K and $T_0 = 750$°K, for different gas concentrations n_0 at the entry, and the corresponding values of the discharge current J_p corresponding to the boundary of transition from the pulsating to steady-state flows. The marker indexes from 1 through 7 along the boundary correspond to different patterns of quasi-stationary flows calculated for $T_0 = 500$°K and the values of J_p and n_0 shown in the table, where the flow rate $\dot m$ (g/s) and parameter β are also presented.

The dashed line in Fig. 4 is described by the equation $\ln J_p = \lambda \ln J_{\dot m} + b$, where $\lambda \approx 0.5$. The condition of steady-state flows of the self-ionizing gas can be formalized in the form of the inequality

$$J_p^2/J_{\dot m} > K, \tag{4.1}$$

where the constant K generally depends on the accelerator channel shape.

Parameters corresponding to quasi-stationary flows on the boundary between the steady-state and pulsating modes

No.	1	2	3	4	5	6	7
$n_0 \times 10^{17}$, cm^{-3}	1.0	1.5	2.0	2.5	3.0	3.5	4.0
J_p, kA	49	63	70	82	85	97	106
$\dot{m} \times 10$, g/s	3.9	6.4	7.8	10	11	14	18
$\beta \times 10^2$	8.0	7.3	7.9	7.2	8.0	7.2	6.9

One may assume that inequality (4.1) is universal and is a consequence, for example, of similarity laws. It is known that the physical pattern of processes is determined by dimensionless parameters rather than by the absolute values, such as J_p, n_0, T_0, and L; i.e., it agrees with similarity criteria. The same dimensionless parameters can correspond to various sets of initial dimensional parameters. For the class of flows considered in this paper, we have two basic dimensionless parameters—ν and β defined by (3.2). As follows from the table, for the set of flows with the same T_0 on the stationarity boundary, it turns out that the dimensionless parameter is almost constant, so that we may assume that $\beta \approx \text{const}$. Similar conclusions are valid for the magnetic viscosity ν or the magnetic Reynolds number Re_m. The distributions of Re_m values along the channel are almost identical in the calculations on the stationarity boundary.

Thus, the flows on the interface between the pulsating and steady-state modes are similar with respect to two dimensionless parameters β and ν. Taking into account their definition (3.2), we conclude that $V_0 = H_0/\sqrt{4\pi\rho_0} \approx \text{const}$ on the interface, at least, for the flows with the same temperature T_0 at the entry. Using the system of equations for steady-state plasma flows in the narrow channel approximation in the absence of dissipation, one can show (see [27]) that the maximum plasma outflow speed at the exit of the accelerator channel is $V_{\max} = \sqrt{2}V_0$. Taking into account the fact that the MHD variables are constant before the ionization front (see Fig. 2), this estimate can be used for the flows of the self-ionizing gas considered in this paper. Simultaneously, we use one more estimate also presented in [27] for the maximum plasma outflow $V_{\max} \sim J_p^2/\dot{m}$ in terms of the discharge current J_p and the mass flux $\dot{m}$. As a result, we have $J_p^2/\dot{m} \sim V_{\max} \sim V_0 \approx \text{const}$ on the boundary between the pulsating and steady-state modes, which agrees with the empirical description.

CONCLUSIONS

Nonstationary pulsating flows of the self-ionizing gas in the channel of a plasma accelerator with an azimuthal magnetic field based on the MHD equations complemented with the equation of kinetics and recombination within the modified diffusion approximation is investigated. The numerical results suggest an empirical condition for the flows of self-ionizing gas to be steady-state; this condition also follows from similarity laws.

ACKNOWLEDGMENTS

This work was supported by the Russian Foundation for Basic Research, project no. 15-01-03085a.

REFERENCES

1. A. I. Morozov, "Principles of coaxial quasi-steady plasma accelerators (QSPAs)," Fiz. Plazmy **16** (2), 131–146 (1990).
2. K. V. Brushlinskii, A. M. Zaborov, A. N. Kozlov, A. I. Morozov, and V. V. Savel'ev, "Numerical simulation of plasma flows in QSPAs," Fiz. Plazmy **16** (2), 147–157 (1990).
3. Ya. F. Volkov, N. V. Kulik, N. V. Marinin, A. I. Morozov, et al., "Analysis of parameters of the plasma flow generated by the full-block QSPA X-50," Fiz. Plazmy **18** (11), 1392–1402 (1992).
4. K. V. Brushlinskii and A. I. Morozov, "Calculation of two-dimensional plasma flows in channels," in *Plasma Physics Problems*, Ed. by M. A. Leontovich (Atomizdat, Moscow, 1974) [in Russian].
5. K. V. Brushlinskii, *Mathematical and Computational Problems of Magnetic Fluid Dynamics* (BINOM Laboratoriya znanii, Moscow, 2009) [in Russian].

6. K. V. Brushlinskii, G. A. Kalugin, and A. N. Kozlov, "Numerical simulation of self-ionizing gas flow in a channel," Preprint No. 50 IPM im. Keldysha, AN SSSR (Moscow, Inst. of Applied Math., USSR Academy of Sciences, 1982).
7. K. V. Brushlinskii, "Numerical simulation of self-ionizing gas flows in channels," in *Two-Dimensional Numerical Plasma Models*, Ed. by N. P. Kozlov and A. I. Morozov (Nauka, Moscow, 1984) [in Russian].
8. K. V. Brushlinskii, "Numerical models of self-ionizing gas flows," in *Encyclopedia of Low-Temperature Plasma*, Ed. by V. E. Fortov (YaNUS-K, Moscow, 2008) [in Russian].
9. A. N. Kozlov, "Two-dimensional nature of the flow instability of gases that are ionized in the channel of a plasma accelerator," Fluid Dyn. **18**, 331–334 (1983).
10. A. N. Kozlov, "Ionization and recombination kinetics in a plasma accelerator channel," Fluid Dyn. **35**, 784–790 (2000).
11. L. M. Biberman, V. S. Vorob'ev, and I. T. Yakubov, *Kinetics of Nonequilibrium Low-Temperature Plasma* (Nauka, Moscow, 1982) [in Russian].
12. A. A. Barmin and A. N. Kozlov, "Structure of the a steady-state ionization front in the plasma accelerator channel," Fluid Dyn. **48**, 556–568 (2013).
13. A. N. Tikhonov, A. A. Samarskii, L. A. Zaklyaz'minskii, et al., "A nonlinear effect of the formation of self-maintaining high-temperature electrically conducting gas layer in unsteady magnetic hydrodynamic processes," Dokl. Akad. Nauk SSSR **173** (4), 808–811 (1967).
14. A. A. Samarskii, S. P. Kurdyumov, Yu. N. Kulikov, L. V. Leskov, Yu. P. Popov, V. V. Savichev, S. S. Filipov, "A magnetohydrodynamic model of unsteady plasma acceleration," Dokl. Akad. Nauk SSSR **206** (2), 307–310 (1972).
15. Ya. B. Zel'dovich and Yu. P. Raizer, *Physics of Shock Waves and High-Temperature Hydrodynamic Phenomena*, Vols. 1 and 2 (Nauka, Moscow, 1966; Academic, New York, 1966, 1967).
16. B. N. Chetverushkin, *Mathematicl Modeling of Radiating Gas Dynamics* (Nauka, Moscow, 1985) [in Russian].
17. A. N. Kozlov, I. E. Garkusha, V. S. Konovalov, and V. G. Novikov, "The radiation intensity of the Lyman alpha line at ionization front in the quasi-steady plasma accelerator," in *Problems of Atomic Science and Technology, Ser. Plasma Physics*, No. 1, 128–130 (2013).
18. A. F. Nikiforov, V. G. Novikov, and V. B. Uvarov, *Quantum-Statistical Models of High-Temperature Plasma* (Fizmatlit, Moscow, 2000) [in Russian].
19. S. I. Braginskii, "Transport phenomena in plasma" in *Plasma Theory Problems,* Ed. by M. A. Leontovich (Atomizdat, Moscow, 1963) [in Russian].
20. V. L. Granovskii, *Electric Current in Gases* (Nauka, Moscow, 1971) [in Russian].
21. A. B. Vatazhin, G. A. Lyubimov, and S. A. Regirer, *Magnetohydrodynamic Flows in Channels* (Fizmatlit, Moscow, 1970) [in Russian].
22. K. V. Brushlinskii, A. P. Favorskii, and A. S. Kholodov, "General notes on numerical methods for solving MHD problems," in *Encyclopedia of Low-Temperature Plasma*, Ed. by V. E. Fortov (Yanus-K, Moscow, 2008) [in Russian].
23. A. G. Kulikovskii, N. V. Pogorelov, and A. Yu. Semenov, *Mathematica Issues of Numerical Solution of Hyperbolic Systems of Equations* (Fizmatlit, Moscow, 2001) [in Russian].
24. E. S. Oran and J. P. Boris, *Numerical Simulation of Reactive Flow* (Elsevier, New York, 1987; Mir, Moscow, 1990).
25. L. M. Degtyarev and A. P. Favorskii, "Flow variant of the sweep method for difference problems with strongly varying coefficients," USSR Comput. Math. Math. Phys. **9**, 285–294 (1969).
26. A. A. Barmin, A. P. Glinov, and A. G. Kulikovskii, "Occurrence of periodic regimes in steady supersonic mid flows due to loss of electrical conductivity of medium," Fluid Dyn. **20**, 613–623 (1985).
27. A. I. Morozov, *Introuction to Plasmadynamics* (Fizmatlit, Moscow, 2008) [in Russian].
28. V. I. Tereshin, A. N. Bandura, O. V. Byrka, V. V. Chebotarev, I. E. Garkusha, I. Landman, V. A. Makhlaj, I. M. Neklyudov, D. G. Solyakov, and A. V. Tsarenko, "Application of powerful quasi-steady-state plasma accelerators for simulation of ITER transient heat loads on divertor surfaces," Plasma Phys. Controlled Fusion **49**, A231–A239 (2007).
29. N. Klimov, V. Podkovyrov, A. Zhitlukhin, D. Kovalenko, B. Bazylev, I. Landman, S. Pestchanyi, G. Janeschitz, G. Federici, M. Merola, A. Loarte, J. Linke, T. Hirai, and J. Compan, "Experimental study of PFCs erosion under ITER-like transient loads at plasma gun facility QSPA," J. Nucl. Mater. **390–391**, 721–726 (2009).
30. V. M. Astashynski, S. I. Ananin, V. V. Askerko, E. A. Kostyukevich, A. M. Kuzmitski, V. V. Uglov, V. M. Anishchik, V. V. Astashynski, N. T. Kvasov, and L. A. Danilyuk, "Materials surface modification using quasi-stationary plasma accelerators," J. Surface Coating Technol. **180–181**, 392–395 (2004).

Translated by A. Klimontovich